THE JOURNAL OF PHYSICAL CHEMISTRY B

Article

pubs.acs.org/JPCB

Why Urease Is a Di-Nickel Enzyme whereas the CcrA β-Lactamase Is a Di-Zinc Enzyme

Crystal E. Valdez and Anastassia N. Alexandrova*

Department of Chemistry and Biochemistry, University of California, Los Angeles, Los Angeles, California 90095-1569, United States

Supporting Information

ABSTRACT: Ureases and metallo-β-lactamases are amide hydrolases closely related in function and structure. However, one major difference between them is that the former uses two nickel cations, and the latter uses two zinc cations to do similar catalytic jobs. What is the reason for this choice that Nature made for the catalytic metals? Is it dictated by electronic or structural reasons in the two catalyzed reactions, or some other evolutionary factors? Are both enzymes "perfect" catalysts, as far as just catalysis is concerned, and if they are, then why? Here, we address these questions through a joint quantum mechanical/molecular mechanical dynamics approach and *ab initio* mechanistic investigation. Five enzyme/substrate systems are considered: urease/urea, CcrA β-lactamase/β-lactam antibiotic model, urease/β-lactam antibiotic model, CcrA β-lactamase/urea, and di-Ni-substituted CcrA β-lactamase/β-lactam antibiotic model. The mechanisms and rates of the metal-facilitated nucleophilic attack are assessed. Both urease and Ni-substituted β-lactamase catalyze the attack on the β-lactam ring with the efficiency surpassing that of natural di-Zn β-lactamase, whereas β-lactamase is unable to hydrolyze urea. These results suggest that in β-lactamases the use of zinc does not provide maximal possible efficiency of the enzyme. Thus, β-lactamases operate by the principle of "good enough"; i.e., the choice for Zn in them leads to a performance that is just satisfactory for its biological purpose but can be evolutionarily improved via replacement of Zn with Ni.

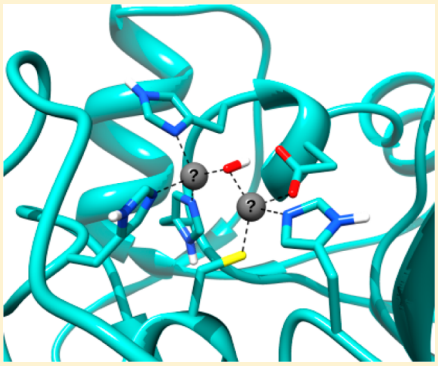

INTRODUCTION

Ureases (EC 3.5.1.5) and metallo-β-lactamases (EC 3.5.2.6) are metallo-enzymes that hydrolyze amides: urea and β-lactam antibiotics, respectively. Urease[1−3] is present in plants, bacteria, and yeast, and converts urea into ammonia and carbon dioxide. Conversion of urea is the last step of nitrogen mineralization in nature. The proficiency of ureases is the highest known among hydrolases.[2,4] It was also suggested that elimination of ammonia from urea may be catalyzed by urease, and the energetics are fairly competitive.[5] Remarkably, urea on its own decomposes exclusively via the deamination route rather than hydrolysis.[4,6] Understanding the functionality of ureases is extremely important, especially in the development of urease inhibitors. Inhibition would reduce the environmental pollution, increase nitrogen uptake in plants, and help the treatment of infections due to ureolytic bacteria.

Ureases are unique among hydrolases in having Ni cations at the active site. They are also Ni-selective *in vivo*, so no Zn-substituted urease can be studied.[7] The presence of Ni in this hydrolase puzzled scientists ever since its discovery.[8] Ni (d^8) is more toxic than Zn (d^{10}), which seems to be the evolutionary force opposing the use of Ni. It was speculated that Ni was required to coordinate simultaneously urea and a water molecule for the reaction, which would cause one of the Ni centers to adopt a coordination close to octahedral, typical for Ni, but atypical for Zn. Thus, a role of the second Ni as a cofactor was speculated. However, it was also shown that water is unlikely to remain in the active site upon the substrate binding.[9] Hence, the choice for Ni in urease remains elusive. At the same time, the catalytic potency of Ni is very high and the proficiency of urease is perhaps attributable to it. From this prospective, we wonder why it is that no other hydrolases use Ni instead of Zn.

β-Lactamases are also amide hydrolases, responsible for antibiotic resistance in pathogenic bacteria.[10−13] They render β-lactam antibiotics ineffective by hydrolyzing the lactam ring. With antibiotic resistance being a major medicinal problem, inhibition of β-lactamases is an active area of research. Among several kinds of β-lactamases, metallo-β-lactamases are the most proficient and hence most problematic enzymes. Metallo-β-lactamases contain two Zn cations in the active site, in contrast to ureases.

Since Ni seems to be a more potent metal, why is it that Zn is chosen in β-lactamases, as well as in many other hydrolases? Is this choice based on maximizing the potency of the enzyme, for not so obvious electronic or structural reasons? Or is this choice an indication of some other evolutionary factors present in cells? Are ureases and β-lactamases "perfect" catalysts? Surely the evolutionary choice could be balanced by a number of biological factors other than enzyme efficiency, such as

Received: March 22, 2012
Revised: July 24, 2012
Published: August 11, 2012

dx.doi.org/10.1021/jp302771n | J. Phys. Chem. B 2012, 116, 10649−10656

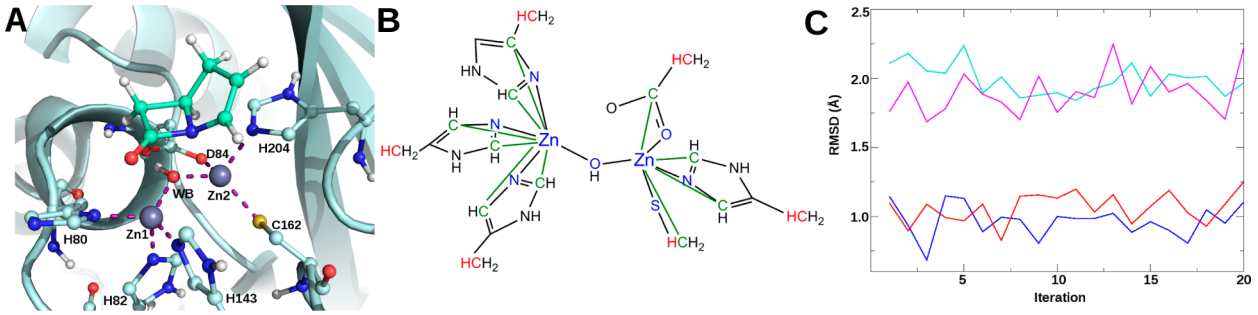

Figure 1. (A) A representative QM/DMD equilibrated structure of β-lactamase with the bound substrate. QM/DMD partitioning is demonstrated. The metal centers and atoms directly coordinated to them are moved only during the QM stage of the simulation. All other atoms shown as sticks can be moved by both QM and DMD. The rest of the protein shown as ribbons is moved exclusively classically by DMD. (B) The green lines show additional constrains that are imposed during the DMD simulation, to retain the chemistry determined at the QM level of theory, the red atoms are frozen during QM calculations, and the blue color marks the atoms in the *QM-only* domain. (C) QM/DMD convergence is demonstrated by the rmsd values for the protein backbone, and the all-atom rmsd of the active site, as a function of iteration number. The teal and blue lines correspond to the protein backbone rmsd and all atom rmsd of the active site, respectively, for the bidentate binding. Similarly, magenta and red correspond to the monodentate binding.

availability of given metals in given organisms, metal toxicity, or the presence of enzyme-building machinery that delivers metals to the active sites. If the catalytic performance is partially sacrificed in this overall evolutionary process, then it would suggest that enzymes could be further improved as catalysts, at least for the use in vitro.

In order to answer the above questions, analysis of the stages of the catalytic mechanism, where the metal plays the crucial role, is needed. There are several proposed mechanisms for both enzymes, with especially vigorous debated points being the group playing the role of the acid in the reaction, the role of the second metal center, the role of the protein flap above the active site, and the overall order of events in the catalytic cycles. However, it is generally agreed upon that one of the metal ions coordinates the substrate via its carbonyl oxygen atom.[2,14−16] The carbonyl group thus gets polarized, and the carbonyl carbon becomes more susceptible to the nucleophilic attack. This pose places the substrate near the nucleophilic OH group bridging the metals (WB). For β-lactamases, the nucleophilic attack by WB is thought to be the first, and, according to some studies, the rate-determining step of hydrolysis.[17−19] Even though a controversy exists about the mechanism of catalytic hydrolysis for ureases,[20] the nucleophilic attack being the first step is still one of the most viable reported possibilities.[21,22] It is additionally supported by the tight binding of inhibitors mimicking the tetrahedral transition state to the urease active site.[23,24] The nucleophilic attack is also the step where the metal plays a major role: coordinating and polarizing the substrate and the nucleophilic water molecule. In this study, we focus on just the attack. We hypothesize that the mechanism and energetics of this step should shed light on the reason for Nature's preference for Zn in β-lactamase and Ni in urease. Our study thus addresses the specific choices for Zn1 and Ni1 in the active sites (metal centers that coordinate the carbonyl carbon) but not necessarily Zn2 and Ni2, although they will appear to play a role too, as will be shown shortly.

In this study, we do not address the substrate binding, and therefore do not assess k_{cat}/K_m (i.e., a typical measure of enzymatic performance). The reason is that both enzymes perform at the diffusion limit, and have solvent-exposed active sites. Thus, the actual event of the substrate binding is not hard. Furthermore, considering our task of realizing the reasons for the metal choices in the two enzymes from the point of view of catalysis, starting from the enzyme−substrate complexes seems reasonable.

This study utilizes a combined statistical mechanical and quantum mechanical approach, for the following reason: As was pointed out,[2,11] the active site and the protein structure at large mutually impact each other in the studied hydrolases, and the overall induced fit upon substrate arrival is expected. As a result, neither pure quantum mechanical studies on cluster models nor classical molecular dynamics simulations of the studied hydrolases are entirely valid, since they produce conflicting ideas about the catalytic mechanisms.[11] Instead, the best approach to study these enzymes would be a combination of quantum mechanics (QM) and classical molecular mechanical (MM) molecular dynamics (MD). However, full QM/MM MD simulations covering nanoseconds of dynamics would be prohibitively expensive, and to date, no QM/MM dynamics studies have been reported for the studied hydrolases. We recently developed a method capable of performing this task, called QM/DMD.[25] Its features include affordable nanosecond time-scale sampling via discrete molecular dynamics (DMD) and QM treatment of the metal containing active site. QM/DMD utilizes a combination of classical dynamics and gradient following relaxation at the QM level, the novel "breathing" QM-DMD boundary, clustering, and annealing. The method was demonstrated to be affordable, balanced, and reliable for modeling of natural and altered metalloproteins.[25] In the present study, we employ QM/DMD to find the preferred docking position of the β-lactam antibiotic model in the CcrA active site, with fully flexible protein. After the docking poses are identified, the mechanistic study is done quantum mechanically, on the cluster models.

THEORETICAL METHODS AND STRUCTURES

Initial Protein Structures and QM/DMD Simulations for β-Lactamase. For urease, the 2.2 Å crystal structure (PDB ID code: 1FWJ)[15] was used to dock urea and prepare the active site model. The 1.85 Å crystal structure of the CcrA β-lactamase (PDB ID code: 1ZNB)[26] was used for the study of this protein. Despite all our efforts, we failed in our search for the bound reactive complex of the chosen truncated model of the β-lactam antibiotic (shown in Figure 1A) and the protein coming directly from the crystal structure. The substrate dissociated away from the active site during geometry

dx.doi.org/10.1021/jp302771n | J. Phys. Chem. B 2012, 116, 10649−10656

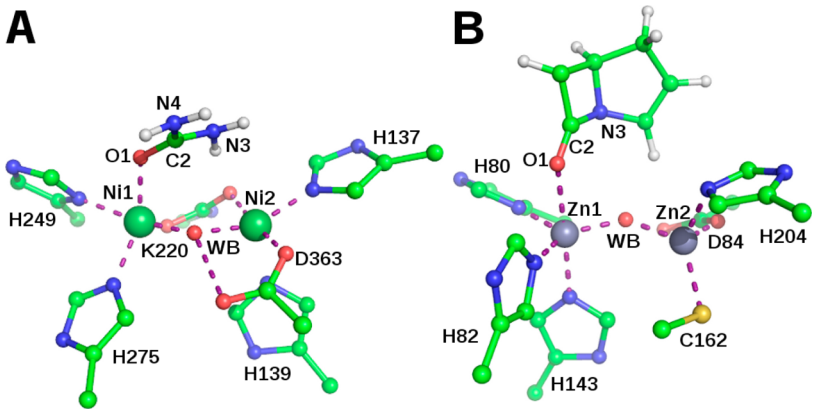

Figure 2. Truncated active sites of (A) urease and (B) βlactamase, used in cluster mechanism studies. The beta carbons of the amino acids are protonated to satisfy all valencies, and fixed at the positions dictated by the rest of the protein.

optimizations. This showed the need for a dynamical docking procedure. We performed it using our newly implemented QM/DMD method.[25]

The specific details of the method are explained elsewhere.[25] In short, QM/DMD is a new mixed quantum mechanical/molecular mechanical method, which features several unique tactics that make it affordable yet reliable on a variety of scales, from large (>10 Å) to small (<1 Å). In QM/DMD simulations, the protein is partitioned into three regions: (1) the QM-only region, consisting of the metals and their immediate coordination sphere, and moved only at the QM level, (2) the larger QM-DMD region, constituting a larger active site (cluster model), and moved by either QM or DMD, depending on the stage of the simulation, and (3) the DMD-only region, which includes the rest of the protein, moved exclusively classically (Figure 1A). QM/DMD simulations proceed in an iterative fashion.

They start with a DMD simulation on the entire protein (i.e., on DMD-only and QM-DMD regions), with frozen metal centers and their immediate coordination environment (QM-only region). A set of additional constrains, as derived from the QM calculations, were imposed to direct the sampling procedure. In particular, for each pair of atoms connected by green lines in Figure 1B, the sampling of the interatomic distance was limited to the interval defined by the QM optimized value ±0.01 Å.

In this way, we avoid the need for parametrization of the classical force field for the metals. The beginning of the DMD simulation is done in conjunction with annealing, used for better sampling, and then the temperature is kept low for the final 10 000 DMD time units (0.5 ns), when the data is collected. This final ensemble of structures is clustered according to a geometric similarity, as follows. The Kabsch[27] rmsd is computed for all pairwise snapshot structures to quantify their geometric similarity. On the basis of the rmsd matrix, a hierarchical clustering algorithm[28] is used to organize all the snapshots in distinct clusters. The user can specify either the number of clusters, or the maximum relative distance (hence the amplitude) within each cluster. For each cluster, a specific representative structure is selected, and one can either choose the structure in the subset closest to the centroid or the structure with the lowest DMD energy. In this study, we requested the number of clusters to be 5, and both the structure closest to the centroid and the one with the lowest energy were used as representatives. Thus, there are 10 structures resultant from the DMD stage of the simulation.

The QM-DMD regions are then cut from those 10 structures. The atoms at the QM-DMD boundary are capped with hydrogen atoms and frozen in Cartesian space to maintain the positions dictated by the protein backbone. Single point QM calculations on these structures are performed at the TPSS[29]/def2-SVP[30] level with an additional empirical dispersion correction,[31] using *TURBOMOLE* v.6.3.[32] A single structure is then chosen on the basis of the combined scoring index (SI) that depends on both the QM and DMD energies, and their differences from the minimum energies found for the given set of structures:

$$SI^i = n(E^i{}_{DMD} - E^{min}{}_{DMD}) + (1 - n)(E^i{}_{QM} - E^{min}{}_{QM})$$

In this work, n is set to 0.5. This structure is then partially optimized at the QM level (for 200 cycles of optimization, after which the optimization is interrupted to save time) and after that uncapped and reinstalled into the protein. The QM-DMD boundary shrinks again, back to the immediate coordination of the metals, and the simulation continues with the second DMD stage, when the geometric information from the active site can propagate to the rest of the protein. The alternating DMD-QM cycle continues for 20 iterations (when the convergence was reached in the present study). The convergence is judged on the basis of the QM and DMD energies of the system, and the rmsd values for the backbone of the protein and the active site (Figure 1C). Two separate QM/DMD simulations were run for the same system: one with a monodentate initial binding pose and one with a bidentate binding pose. Both binding poses retained the initial coordination, indicating that both are minima on the QM/DMD potential energy surface. The result is in agreement with earlier mechanistic studies on cluster models,[20g] which means that the role of the protein in the structure of the substrate-active site complex is minor. The bidentate pose yields the structure in the reactive orientation and overall lower QM and DMD energies.

From the equilibrated protein with the substrate coordinated in the bidentate fashion, a single structure with the lowest combined QM and DMD energy was chosen for the mechanistic study. That representative structure yielded by QM/DMD is shown in Figure 1A. QM/DMD was able to bind the carbonyl O atom of the substrate to the Zn1 center, with a bond length R(O−Zn1) of 3.7 Å. The nucleophilic O of WB

dx.doi.org/10.1021/jp302771n | J. Phys. Chem. B 2012, 116, 10649−10656

was located 3.7 Å from the carbonyl C. The binding mode was monodentate.

The Ni-substituted β-lactamase was obtained by replacing Zn with Ni and optimizing the complex with the substrate bound, exclusively at the QM level. The overall structure did not change significantly, and docking was straightforward. Additionally, we studied a complex of β-lactamase with urea. Urea, being a small molecule, fits in the active site of β-lactamase without problems. No QM/DMD sampling was required for these two systems.

Active Site Complexes. For the mechanistic study, all active site amino acid residues were truncated at the beta carbons and capped with hydrogens. These carbon atoms were fixed, preserving the backbone structure of the complexes. The urease active site (Figure 2A) contains two pseudo-octahedral Ni atoms: Ni1 is coordinated to residues H249, H275, a carbamylated lysine (K220), a water molecule (W1), and bridging water (WB); Ni2 is coordinated to H137, H139, D363, a water molecule (W2), the bridging water (WB), and carbamylated lysine (K220) coordinated to Ni1. As based on the crystallographic structure of the DAP inhibited urease (PDB code 3UBP),[23] the bidendate binding nature of urea displaces W1 and W2 coordinated to the nickels, a binding pose suggested to mimic a transition state.[9] Benini et al.[23,24] proposed hydrolysis of urea to occur with nucleophilic attack of bridging hydroxide, with necessary bidentate ligation of urea to the two electrophilic nickel ions, due to the close proximity of urea to the bridging hydroxide. Hence, W1 and W2 were removed from the complex (Figure 2A).

We tested different spin states of the dinickel complexes, and found that the high-spin quintet state is lowest in energy (triplet was ∼9 kcal/mol higher in energy). This is in agreement with previous theoretical and experimental reports.[20] The active site of ureases is not EPR detectable. However, magnetic measurements on jack bean urease have been performed, and showed that the active site is mostly high spin, with some spin heterogeneity being required for the best fit with experimental data.[20a−f] Thus, the ideal theoretical study would address the mixed-spin state by multireference calculations. However, this is prohibitively expensive for the bimetallic active site of ureases. Hence, the adopted broken-symmetry approach appears to be the best, and it showed the high spin complex being of the lowest energy. Additionally, in a recent theoretical study on the model complex, the quintet also was found to be the lowest energy state.[20g] Thus, we further considered only the quintet.

All spectroscopic and structural data point at the fact that both Ni centers are in the formal oxidation state of +2 in ureases. Hence, the charge on the complex was +1, and no other charge states were considered.

The β-lactamase active site (Figure 2B) contains a tetrahedrally coordinated Zn1 with three histidine residues (H80, H82, and H143) and bridging water (WB) and a bypyramidal Zn2 coordinated by D84, C162, and H204, the bridging water coordinated to Zn1 (WB), and an additional water molecule (W2). W2 is speculated to be readily displaced by the β-lactam ring nitrogen, facilitating the hydrolysis, as suggested by Merz et al.[33] Thus, W2 was removed. The protonation state of D103 in CcrA was questioned in the past, and it was linked to the stability of the Zn−OH−Zn bridge. Results of classical MD simulations suggested that protonated D103 yields a looser bridge and higher activity of the enzyme.[33,34] However, it was shown that both forms have similar activities predicted computationally, and thus in this study, D103 was chosen to be deprotonated, in agreement with Merz and co-workers.[20g] The spin of the active site is zero, and the total charge is +1. From our theoretical assessment, the active site of the Ni-substituted β-lactamase was a quintet state, charged +1 as well.

All cluster studies were done at the TPSS/def2-SVP and B3LYP[35]/def2-SV(P) levels with empirical dispersion correction, using *TURBOMOLE*. Geometry optimizations of the reactants, transition states (TSs), and intermediates were carried out. All TSs and minima were confirmed by frequency calculations. Each TS had only one imaginary frequency, corresponding to the normal mode coinciding with the reaction coordinate.

RESULTS AND DISCUSSION

In order to explore the role of the metals in the nucleophilic attack on the carbonyl group in hydrolysis, five enzyme/substrate systems were considered: urease/urea, urease/β-lactam, β-lactamase/urea, β-lactamase/β-lactam, and di-Ni-substituted β-lactamase/β-lactam. Our starting reasoning reads as follows: β-lactam is likely easier to hydrolyze than urea, due to the high strain in the four-membered ring, and the diminished resonance stabilization as compared to that in urea. At the same time, Ni is likely a more catalytically potent metal than Zn in this reaction. Therefore, it seems like the nucleophilic attack in urease should be more easily accomplished on β-lactam than on urea, if the structure of the active site of urease otherwise permits. On the other hand, hydrolysis of both substrates should be more easily done by urease than by β-lactamase. Finally, urea should be less eagerly, if at all, hydrolyzed by β-lactamase. Additionally, there is a possibility that the overall structure of the urease active site is suboptimal for β-lactam binding. Hence, we also consider Ni-substituted β-lactamase, with the aim to combine the seemingly more potent metal with the protein structure optimal for binding β-lactam, to complete the picture. In this study, we are effectively on the hunt for the facts that would break the elementary logics outlined in this paragraph, which would thereby reveal some hidden evolutionary reasons for the metal selection for catalysis performed by the two studied hydrolases.

Figure 3 and Table 1 show the reaction profiles and associated energetics for the nucleophilic attack on two substrates catalyzed by urease. For both substrates, the binding starts from monodentate coordination of the carbonyl O to Ni1, and then evolves into the bidentate coordination where the amide N of the substrate attaches to Ni2. The energy goes down upon bidentate coordination for both substrates. The nucleophilic attack by O_{WB} then takes place. The barrier to this process is 14.3 kcal/mol for urea, in a reasonable agreement with previous studies.[36] As expected, the barrier toward the nucleophilic attack on β-lactam is smaller than that on urea by ca. 6.8 kcal/mol. Both systems end up in the tetrahedral intermediates, which would undergo further decomposition through protonation of the amide N2 atoms and cleavage of the C2−N3 bonds. This subsequent step is more complicated, and details of various possible reaction routes are extensively described and debated in the literature. Here, we do not consider reaction mechanisms any further, as justified in the Introduction. Our goal is to reveal the preference for Ni and Zn in these two hydrolases, and this should be seen from the nucleophilic attack step alone.

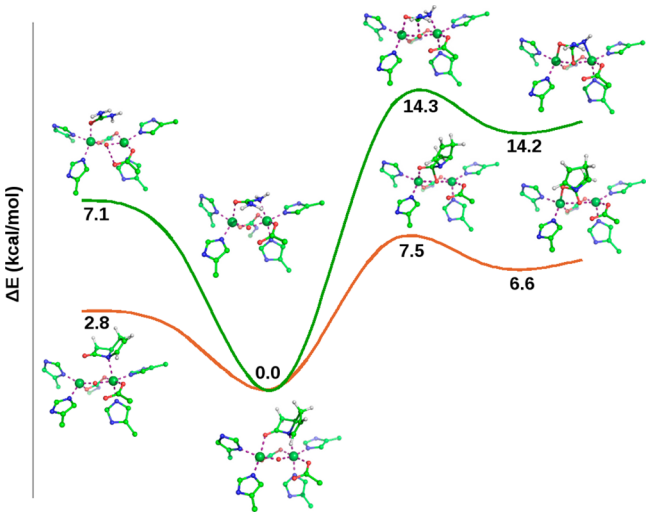

Figure 3. Reaction profile of nucleophilic attack catalyzed by urease with urea (green line) and β-lactam antibiotic model (orange line), in reference to bidentate coordination of substrates to nickel atoms. Most of the hydrogen atoms are omitted for clarity. All energies are ZPE-corrected.

Table 2 illustrates the characteristic geometric parameters in the active site, and their evolution from the reactants, to the TS, and then to the tetrahedral intermediate. As the substrates bind to urease, and go into the bidentate coordination, the Ni1−O1 becomes longer (2.1−2.3 Å), allowing ideal positioning for Ni2−N3 coordination. This tight coordination to Ni1 also persists throughout the nucleophilic attack step. Upon binding of the substrates, the carbonyl C−O bond distances (R(O1−C2)) elongate slightly, by 0.02−0.04 Å, as compared to those in the unbound substrates, and become significantly longer once the attack is accomplished. Binding to Ni1 and activation of carbonyl are very similar between the two substrates. Therefore, the smaller barrier to the reaction in the case of β-lactam is due solely to the properties of the β-lactam molecule (high strain, reduced π-resonance). The C2 and O_{WB} atoms are found to be in reactive orientations in the starting complexes, and naturally, R(C2−O_{WB}) becomes shorter in the course of the reaction. For urea, the TS happens relatively late, at smaller R(C2−O_{WB}), which correlates with the higher barrier to the reaction, and the tetrahedral intermediate corresponds to a very shallow and high energy minimum on the potential energy surface. For β-lactam, the TS is early, at a longer R(C2−O_{WB}). There is a lower barrier to the reaction and the intermediate is more stable.

Now, let us consider hydrolysis of the two substrates by the CcrA β-lactamase, in its natural di-Zn form and in the di-Ni-substituted form. Figure 4 shows the reaction profiles for the nucleophilic attack occurring in these systems and Table 6 gives the important interatomic distances. In this case, the system still evolves from monodentate to bidentate coordination, which in turn precedes the attack. However, the bidentate complexes are higher in energy than the monodentate ones for the natural di-Zn enzyme, possibly due to the lower affinity of Zn to the electrophilic groups of the substrates, as compared to Ni. The TS for urea hydrolysis is high in energy (19.6 kcal/mol), and definitely much higher than when this reaction is catalyzed by urease, as expected. For β-lactam, the reaction barrier is 15.7 kcal/mol. Apparently, β-lactamase is unable to outdo urease in facilitating the nucleophilic attack on β-lactam, which at least in part is attributable to the higher potency of Ni1. However, one must also remember that the active site of urease is probably suboptimal for binding the TS of a large β-lactam containing molecule. In order to account for this latter effect, we considered Ni-substituted β-lactamase. Replacing Zn with Ni in the β-lactamase active site leads to the reduction of the barrier to the attack. As anticipated, di-Ni-substituted β-lactamase is the strongest catalyst for the nucleophilic attack on β-lactam. Furthermore, it is known that the nucleophilic attack is also the rate determining step of enzymatic hydrolysis of β-lactam.[18−20] The product of the nucleophilic attack is lower than that for the native β-lactamase. Therefore, our results suggest that having Ni in the active site of β-lactamase would be better for both the nucleophilic attack and overall enzyme performance than having Zn.

To support the qualitative observations presented in the previous paragraph, geometric parameters characteristic of the nucleophilic attack on the two substrates catalyzed by β-lactamases are shown in Tables 3 and 4. Overall, the parameters of the active site and the substrate are similar to those observed in the case of urease. The coordination to Zn1 is looser, as judged from the longer R(Zn1−O1). However, the carbonyl group still gets elongated and thus activated. This activation is stronger for β-lactam than for urea. The C2 and O_{WB} atoms arrange into reactive mutual orientations at bidentate coordination. R(C2−O_{WB}) in the bidentate complex for β-lactam is longer than that for urea. Not surprisingly, urea is a smaller molecule then the lactam antibiotic model, and when arranged in the bidentate mode coordination with a short N3−Zn2 bond, it comes in close proximity to WB. The TS for β-lactam happens later, in terms of R(C2−O_{WB}), which could be viewed as the reaction coordinate. According to our calculations, a tetrahedral intermediate minimum does not exist for the β-lactamase/urea complex. Instead, when the normal mode of the imaginary frequency in the TS is followed toward the products of the nucleophilic attack, the substrate detaches from the active site and the system evolves back to the unbound reactants. In fact, the very existence of the TS may be an artifact of the harmonic approximation in calculations of vibrational frequencies. Nevertheless, considering the energetics of the process, this result suggests that β-lactamase is unable to hydrolyze urea.

Table 5 contains analogous data on the Ni-substituted β-lactamase. The properties of this active site appear to be similar to those of di-Zn β-lactamase. The only prominent differences include tighter binding of the substrate to Ni1, tighter Ni1−OH−Ni2 bridge, a slightly longer C2−O_{WB} distance, and a slightly shorter C2−N3 distance in the intermediate. Overall,

Table 1. Relative Free Energy (kcal/mol) for the Urease Systems (See Figure 3)

	urease/urea				urease/β-lactam			
	monodentate	bidentate	TS	interm.	monodentate	bidentate	TS	interm.
TPSS/def2-SVP	7.1	0.0	14.3	14.2	2.8	0.0	7.5	6.6
B3LYP/def2-SV(P)	5.9	0.0	17.8	17.7	1.8	0.0	12.2	9.6

dx.doi.org/10.1021/jp302771n | J. Phys. Chem. B 2012, 116, 10649−10656

Table 2. Interatomic Distances for the Nucleophilic Attack Catalyzed by Urease, for Urea and β-Lactam, in Å, with TPSS/def2-SVP and B3LYP/def2-SV(P) (in Parentheses)[a]

	Urea				β-lactam			
	monodentate	bidentate	TS	interm.	monodentate	bidentate	TS	interm.
Ni1−O1	2.11 (2.11)	2.31 (2.31)	2.06 (2.06)	2.03 (2.03)	3.01 (2.94)	2.22 (2.26)	2.09 (2.07)	2.08 (1.96)
O1−C2	1.26 (1.26)	1.25 (1.25)	1.31 (1.30)	1.32 (1.32)	1.21 (1.20)	1.22 (1.21)	1.28 (1.27)	1.40 (1.33)
C2−O_{WB}	2.81 (2.09)	2.57 (2.57)	1.69 (1.71)	1.61 (1.61)	2.95 (2.98)	2.97 (3.00)	1.78 (1.82)	1.59 (1.51)
C2−N3	1.36 (1.36)	1.40 (1.40)	1.47 (1.47)	1.48 (1.48)	1.44 (1.43)	1.41 (1.41)	1.44 (1.43)	1.47 (1.50)
N3−Ni2	3.08 (3.08)	2.25 (2.25)	2.13 (2.16)	2.12 (2.12)	2.43 (2.45)	2.46 (2.49)	3.77 (3.88)	3.77 (3.98)
Ni1−O_{WB}	1.96 (1.96) 2.15[b] 1.991[c]	1.91 (1.91)	2.08 (2.06)	2.11 (2.11)	1.87 (1.88)	1.91 (1.91)	2.08 (2.07)	2.01 (2.18)
O_{WB}−Ni2	1.93 (1.93) 1.98[b] 2.071[c]	1.97 (1.97)	2.05 (2.06)	2.06 (2.06)	1.97 (1.98)	1.99 (1.99)	2.01 (2.02)	2.16 (2.05)
Ni1−Ni2	3.51 (3.51) 3.59[b] 3.557[c]	3.43 (3.43)	3.63 (3.64)	3.66 (3.66)	3.44 (3.48)	3.44 (3.46)	3.63 (3.63)	3.63 (3.65)

[a]All atoms are numbered as in Figure 2. [b]Structural data compared to the X-ray structure of native urease (PDB 1FWJ) that does not contain substrate. [c]Structural data compared to cluster calculations from ref 35 that do not contain substrate.

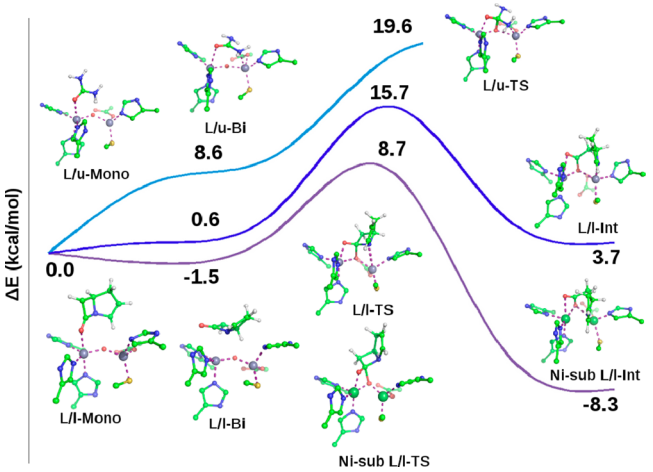

Figure 4. Reaction profile of nucleophilic attack catalyzed by β-lactamase with urea (light blue line), and β-lactam molecule (dark blue line), and Ni-substituted β-lactamase with β-lactam (purple line). Energies are shown relative to the monodentate complexes, and are ZPE-corrected. Structures for Ni-substituted lactamase are similar to di-Zn β-lactamase, and were omitted for clarity, except for the intermediate, which is different in the two enzymes. Most of the hydrogen atoms are omitted for clarity.

this correlates with the expected stronger electrophilic character of Ni versus Zn.

There is one critical difference to be observed between the ways that all three proteins interact with β-lactam. In natural and Ni-substituted β-lactamases, as soon as the attack on the carbonyl is complete, the C2−N3 bond splits spontaneously. This effect is not observed for urease but is prominent for both β-lactamases. In natural β-lactamase, it is additionally facilitated by the weakness of the Zn1−OH−Zn2 bridge. Notice that O_{WB}−Zn2 and O_{WB}−Ni2 both increase significantly when the nucleophilic attack is complete. The Zn2−N3 distance in β-lactamase is comparable to the Ni2−N3 bond in the Ni-substituted enzyme. Recalling that the nucleophilic attack is the rate determining step in the hydrolysis of β-lactam,[17−19] the subtle energy difference between the tetrahedral intermediates in the two β-lactamases is probably unimportant for the overall performance of the enzymes.

On the other hand, apparently, the active site of urease is not suited for the splitting of the C2−N3 bond in β-lactam. At the same time, the C2−N3 bond is stronger in urea, so no active site can split it spontaneously. This agrees with the previous reports suggesting that the splitting of the C2−N3 bond and elimination of ammonia is the rate-determining step of enzymatic hydrolysis of urea.

To summarize this section, we infer that having Ni in the active site of hydrolases is probably better for the overall enzymatic performance than having Zn. At least the nucleophilic attack on the substrate is much more strongly facilitated by Ni.

DISCUSSION AND CONCLUSIONS

This theoretical study explored the possible catalytic mechanistic reasons for the evolutionary choice of metals in two amide hydrolases: urease and β-lactamase. The active sites of these enzymes are similarly structured, except that the former uses two Ni cations and the latter uses two Zn cations to catalyze very similar reactions. Urease is unique among hydrolases to use Ni, and that puzzled the scientific community since the discovery of urease. However, from the inferred

Table 3. Relative Free Energy (kcal/mol) for the β-Lactamase Systems (See Figure 4)

	β-lactamase/urea				β-lactamase/β-lactam			
	monodentate	bidentate	TS	interm.	monodentate	bidentate	TS	interm.
TPSS/def2-SVP	0.0	8.6	19.6	n/a[a]	0.0	0.6	15.7	3.7
B3LYP/def2-SV(P)	0.0	9.3	29.2		0.0	0.1	18.4	2.2

[a]See text for details.

dx.doi.org/10.1021/jp302771n | J. Phys. Chem. B 2012, 116, 10649−10656

Table 4. Interatomic Distances for the Nucleophilic Attack Catalyzed by β-Lactamase, for Urea and β-Lactam, in Å, with TPSS/def2-SVP and B3LYP/def2-SV(P) (in Parentheses)[a]

	urea				β-lactam			
	monodentate	bidentate	TS	interm.	monodentate	bidentate	TS	interm.
Zn1−O1	2.47 (2.47)	2.68 (2.81)	2.13 (2.17)	n/a[b]	2.35 (2.39)	3.77 (3.75)	2.04 (2.01)	2.40 (2.48)
O1−C2	1.25 (1.25)	1.24 (1.23)	1.29 (1.28)		1.23 (1.22)	1.22 (1.21)	1.30 (1.30)	1.24 (1.23)
C2−O_{WB}	3.32 (3.32)	2.68 (2.74)	1.66 (1.66)		3.43 (3.45)	3.76 (3.75)	1.57 (1.53)	1.35 (1.33)
C2−N3	1.36 (1.36)	1.41 (1.40)	1.51 (1.50)		1.38 (1.38)	1.40 (1.40)	1.52 (1.50)	2.72 (2.84)
Zn1−O_{WB}	1.94 (1.94)	1.89 (1.89)	2.04 (2.02)		1.90 (1.90)	1.89 (1.89)	2.13 (2.13)	2.03 (2.01)
N3−Zn2	3.84 (3.84)	2.43 (2.50)	2.14 (2.15)		4.52 (4.53)	4.19 (4.14)	2.86 (2.95)	1.96 (1.91)
O_{WB}-Zn2	2.01 (2.01)	1.99 (1.99)	2.30 (2.29)		1.96 (1.96)	1.97 (1.97)	2.06 (2.08)	2.21 (2.31)
Zn1−Zn2	3.67 (3.67)	3.63 (3.63)	4.02 (3.97)		3.49 (3.51)	3.44 (3.46)	3.59 (3.65)	3.33 (3.74)

[a]All atoms are numbered as in Figure 4. [b]See text for details.

Table 5. Relative Free Energy (kcal/mol) for the Ni-Substituted β-Lactamase Systems (See Figure 4) Where the Thermal Correction Was Added to the TPSS/def2-SVP Data

	monodentate	bidentate	TS	interm.
TPSS/def2-SVP	0.0	−1.5	8.7	−9.3
B3LYP/def2-SV(P)	0.0	−0.9	12.4	−4.8

Table 6. Interatomic Distances for the Nucleophilic Attack on β-Lactam Catalyzed by Ni-Substituted β-Lactamase, in Å[a]

	monodentate	bidentate	TS	interm.
Ni1−O1	2.30 (2.24)	3.69 (3.73)	2.11 (2.03)	2.36 (2.42)
O1−C2	1.23 (1.22)	1.21 (1.20)	1.27 (1.30)	1.25 (1.24)
C2−O_{WB}	3.20 (3.24)	3.66 (3.83)	1.80 (1.54)	1.32 (1.31)
C2−N3	1.38 (1.37)	1.44 (1.43)	1.44 (1.48)	2.58 (2.62)
Ni1−O_{WB}	1.92 (1.91)	1.91 (1.91)	1.96 (2.03)	2.14 (2.11)
N3−Ni2	4.23 (4.34)	3.66 (3.90)	3.49 (3.47)	1.99 (2.02)
O_{WB}−Ni2	1.97 (1.99)	1.96 (1.99)	1.98 (2.06)	2.52 (2.73)
Ni1−Ni2	2.90 (3.23)	2.89 (3.25)	2.76 (2.88)	3.03 (3.14)

[a]All atoms are numbered as in Figure 2, except that Zn1 is now Ni1 and Zn2 is Ni2.

higher catalytic potency of Ni, we rather wondered why no more hydrolases use Ni, and why the seemingly less potent Zn cation is often used instead. We do not address all the factors present in the cell that may put pressure on the specific choice for the metal. Rather, we would like to know if the mechanism and rate of the catalyzed reactions are fully optimized with the given choice for the metals, or if instead they are compromised.

We considered the first step of hydrolysis, the nucleophilic attack, in which the metal center should play the key role of positioning and activating the carbonyl group of the substrates. We considered the hydrolysis of urea and a mimic of a β-lactam antibiotic in the active sites of urease, β-lactamase, and Ni-substituted β-lactamase. We found that β-lactam is most easily hydrolyzed by Ni-substituted β-lactamase, exhibiting the lowest barrier to the nucleophilic attack, and also the spontaneous splitting of the C2−N3 bond in the substrate, after the attack. The latter is also characteristic of di-Zn β-lactamase, but the barrier to the attack is higher. The barrier in urease is smaller than that in natural β-lactamase, but the C2−N3 bond does not spontaneously open in the urease active site. On the other hand, hydrolysis of urea in di-Zn β-lactamase is unfeasible. Thus, hydrolysis of urea requires Ni, and cannot be done with Zn, but hydrolysis of β-lactam can benefit from the presence of Ni rather than Zn at the active site.

Nature's preference for Zn over Ni in the active site of β-lactamase may be dictated by other factors in the cell, such as higher toxicity or lower availability of Ni. On the other hand, considering the already high performance of di-Zn β-lactamases in hydrolyzing β-lactam, it is possible that they are simply "good enough" as catalysts, while they satisfy other requirements present in the cell, so no further optimization by metal substitution was pursued. From the fundamental prospective of protein science, this suggests that natural enzymes could be further improved, especially if the intention is to use them for catalysis *in vitro*, rather than *in vivo*. This message is also of interest to the field of artificial enzyme design.

■ ASSOCIATED CONTENT

Supporting Information

Reaction free energies and the method of calculating entropic contributions for the constrained complexes. This material is available free of charge via the Internet at http://pubs.acs.org.

■ AUTHOR INFORMATION

Corresponding Author

*E-mail: ana@chem.ucla.edu.

Notes

The authors declare no competing financial interest.

■ ACKNOWLEDGMENTS

This work was supported by the DARPA Young Faculty Award N66001-11-1-4138 (ANA) and the NSF Graduate Fellowship #2011115747 (CEV).

■ REFERENCES

(1) Zambelli, B.; Musiani, F.; Benini, S.; Ciurli, S. *Acc. Chem. Res.* **2011**, *44*, 520−530.
(2) Karplus, P. A.; Pearson, M. A.; Hausinger, R. P. *Acc. Chem. Res.* **1997**, *30*, 330−337.
(3) Krajewska, B. *J. Mol. Catal. B* **2009**, *59*, 9−21.
(4) Callahan, B. P.; Yuan, Y.; Wolfenden, R. *J. Am. Chem. Soc.* **2005**, *127*, 10828−10829.
(5) Estiu, G.; Merz, K. M. *J. Am. Chem. Soc.* **2004**, *126*, 11832−11842.
(6) Alexandrova, A. N.; Jorgensen, W. L. *J. Phys. Chem. B* **2007**, *111*, 720−730.
(7) Zambelli, B.; Danielli, A.; Romagnoli, S.; Neyroz, P.; Ciurli, S.; Scarlato, V. *J. Mol. Biol.* **2008**, *383*, 1129−1143.
(8) Dixon, N. E.; Gazzola, C.; Blakeley, R.; Zerner, B. *J. Am. Chem. Soc.* **1975**, *97*, 4131−4132.
(9) Ciurli, S.; Benini, S.; Rypniewski, W. R.; Wilson, K. S.; Miletti, S.; Mangani, S. *Coord. Chem. Rev.* **1999**, *190−192*, 331−355.
(10) Page, M. I. *The Chemistry of β-Lactams*; Blackie: London, 1992.

(11) Estiu, G.; Suárez, D.; Merz, K. M. *J. Comput. Chem.* **2006**, *27*, 1240−1262.
(12) Lipscomb, W. N.; Sträter, N. *Chem. Rev.* **1996**, *96*, 2375−2433.
(13) T. Abraham, E. P.; Waley, S. G. In *The β-Lactamase*; Hamilton-Miller, J. M. T., Smith, J. T., Eds.; Academic Press: London, 1979; pp 311−338.
(14) Jabri, E.; Carr, M. B.; Hausinger, R. P.; Karplus, P. A. *Science* **1995**, *268*, 998−1004.
(15) Pearson., M. A.; Michel, L. O.; Hausinger, R. P.; Karplus, P. A. *Biochemistry* **1997**, *36*, 8164−8172.
(16) Park, H.; Brothers, E. N.; Merz, K. M. *J. Am. Chem. Soc.* **2005**, *127*, 4232−4241.
(17) Krauss, M.; Gresh, N.; Antony, J. *J. Phys. Chem. B* **2003**, *107*, 1215−1229.
(18) Estiu, G.; Suárez, D.; Merz, K. M. *J. Comput. Chem.* **2007**, *27*, 1240−1262.
(19) Xu, D.; Guo, H.; Cui, Q. *J. Am. Chem. Soc.* **2007**, *129*, 10814−10822.
(20) (a) Wilcox, D. E. *Chem. Rev.* **1996**, *96*, 2435−2458. (b) Clark, P. A.; Wilcox, D. E. *Inorg. Chem.* **1989**, *28*, 1326−1333. (c) Dixon, N. E.; Gazzola, C.; Asher, C. J.; Lee, D. S. W.; Blakeley, R. L.; Zerner, B. *Can. J. Biochem.* **1980**, *58*, 474−480. (d) Blakeley, R. L.; Dixon, N. E.; Zerner, B. *Biochim. Biophys. Acta* **1983**, *744*, 219−229. (e) Clark, P. A.; Wilcox, D. E. *Inorg. Chem.* **1989**, *28*, 1326−1333. (f) Day, E. P.; Peterson, J.; Sendova, M. S.; Todd, M. J.; Hausinger, R. P. *Inorg. Chem.* **1993**, *32*, 634−638. (g) Suarez, D.; Diaz, N.; Merz, K. M. *J. Am. Chem. Soc.* **2003**, *125*, 15324−15337.
(21) Musiani, F.; Arnold, E.; Casadio, R.; Ciurli, S. *J. Biol. Inorg. Chem.* **2001**, *6*, 300−314.
(22) Pearson, M. A.; Park, I.-S.; Schaller, R. A.; Michel, L. O.; Karplus, P. A.; Hausinger, R. P. *Biochemistry* **2000**, *39*, 8575−8584.
(23) Benini, S.; Rypniewski, W. R.; Wilson, K. S.; Miletti, S.; Ciurli, S.; Mangani, S. *Struct. Folding Des.* **1999**, *7*, 205−216.
(24) Benine, S.; Rypniewski, W. R.; Wilson, K. S.; Miletti, S.; Ciurli, S.; Mangani, S. *Structure* **1999**, *7*, 205−216.
(25) Sparta, M.; Ding, F.; Shirvanyants, D.; Dokholyan, N. V.; Alexandrova, A. N. *Biophys. J.* **2012**, *103*, 767−776.
(26) Concha, N. O.; Rasmussen, B. A.; Bush, K.; Herzberg, O. *Structure* **1996**, *4*, 823−836.
(27) Kabsch, W. *Acta Crystallogr., Sect. A* **1976**, *32*, 922−923.
(28) Barton, G. J. *OC - A cluster analysis program*; University of Dundee: Scotland, U.K., 1993, 2002; http://www.compbio.dundee.ac.uk/downloads/oc.
(29) (a) Perdew, J. P.; Wang, Y. *Phys. Rev. B* **1992**, *45*, 13244−13249. (b) Tao, J.; Perdew, J. P.; Staroverov, V. N.; Scuseria, G. E. *Phys. Rev. Lett.* **2003**, *91*, 146401−146404.
(30) Schafer, A.; Horn, H.; Ahlrichs, R. *J. Chem. Phys.* **1992**, *97*, 2571−2577.
(31) Grimme, S. *J. Comput. Chem.* **2004**, *25*, 1463−1473.
(32) Ahlrichs, R.; Bär, M.; Häser, M.; Horn, H.; Kölmel, C. *Chem. Phys. Lett.* **1989**, *162*, 165−169.
(33) Diaz, N.; Suárez, D.; Merz, K. M. *J. Am. Chem. Soc.* **2000**, *122*, 4197−4208.
(34) Suárez, D.; Brothers, E. N.; Merz, K. M. *Biochemistry* **2002**, *41*, 6615−6630.
(35) (a) Parr, R. G.; Yang, W. *Density-functional theory of atoms and molecules*; Oxford Univ. Press: Oxford, U.K., 1989. (b) Becke, A. D. *J. Chem. Phys.* **1993**, *98*, 5648. (c) Perdew, J. P.; Chevary, J. A.; Vosko, S. H.; Jackson, K. A.; Pederson, M. R.; Singh, D. J.; Fiolhais, C. *Phys. Rev. B* **1992**, *46*, 6671.
(36) Suarez, D.; Diaz, N.; Merz, K. M. *J. Am. Chem. Soc.* **2003**, *125*, 15324−15337.